Optics Communications 97 (1993) 115–129
North-Holland

OPTICS
COMMUNICATIONS

Full length article

Triplator – optical signal processor based on rotational shearing interferometer

Joseph Rosen
Rome Laboratory, Optical Signal Processing Branch/EROP, Hanscom AFB, MA 01731-5000, USA

and

Joseph Shamir
Department of Electrical Engineering, Technion – Israel Institute of Technology, Haifa 32000, Israel

Received 25 June 1992; revised manuscript received 30 September 1992

A new integral transform involving three functions, a triplation, is introduced and its optical implementation is demonstrated. The optical system is based on a rotational shearing interferometer illuminated by partially coherent light. The triplation operation is analyzed theoretically and some of its possible applications are discussed.

1. Introduction

In a recent publication [1] a generalized interferometric signal processor was introduced. In this processor a Fourier hologram is recorded by a rotational shearing interferometer and reconstructed by a conventional coherent 2-f optical Fourier transform (FT) configuration. It has been shown that a nonconventional processor could be obtained which involved three arbitrary complex functions. In some special cases and under various conditions, the system becomes an efficient image processor for specific tasks. For instance, the system can be used as a joint transform correlator (JTC) [2] illuminated by spatially incoherent light. In this paper we consider more extensively the case of the generalized processor from a theoretical point of view and demonstrate its operation experimentally. In the general case, three functions may be involved in some mathematical operation, which can be degenerated to more familiar operations, like convolution or multiplication between two functions. The initial goal of this work was to investigate various effects and processes that were discovered during previous work. One of these was the implementation of some unusual mathematical transformation with a slightly modified rotational shearing interferometer. The main purpose of this paper is to introduce this transform, and to consider its principal properties. Although the full merits of this transformation are not clear yet, some possible application will be briefly discussed and summarized in the conclusions. One particularly interesting application is described in sec. 4 while some special cases are considered in sec. 6. Preliminary experimental results are given in sec. 5. We start the analysis with a description of the optical system, which executes this processing.

2. The optical system

The optical system is composed of a rotational shearing interferometer illuminated by a spatially incoherent quasi-monochromatic light source [3], as shown in fig. 1. Three functions are involved in the process. Two

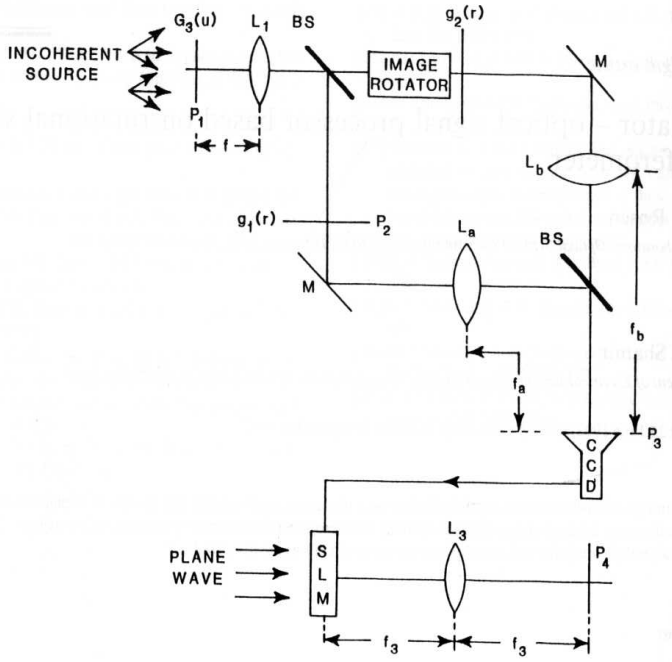

Fig. 1. Rotational shearing interferometer which is designed to perform the triplation.

of them, $g_1(\boldsymbol{r})$ and $g_2(\boldsymbol{r})$, may be general complex functions placed in the input planes, P_2, of the two interferometer channels. The third function, $G_3(\xi)$, is the intensity distribution of a spatially incoherent light source in plane P_1, and is therefore restricted to positive values. Since plane P_3 is in the focal plane of the lenses L_a and L_b, it is considered as a Fourier plane related to plane P_2. In one channel of the interferometer there are two periscopes [4], that serve to rotate the light distributions in the two channels with respect to each other, by an angle π. Every point in the source generates a plane wave of relative amplitude $\sqrt{G_3(\xi)}$ propagating at an angle $\sin^{-1}(\xi/f_1)$ in one channel and $\sin^{-1}(-\xi/f_1)$ in the other, relative to the optical axis. These planes waves are multiplied by $g_1(\boldsymbol{r})$ in one channel, and by $g_2(\boldsymbol{r})$ in the other. The overall intensity distribution over plane P_3 is obtained by a coherent superposition of the complex amplitudes form each source point propagated through the two channels and a summation over all the independent source points:

$$I(\rho)=\int_{\Xi}\mathrm{d}^2\xi\left|\int_{R}\mathrm{d}^2\boldsymbol{r}\sqrt{G_3(\xi)}\exp\left(-\mathrm{i}\frac{2\pi}{\lambda f_1}\xi\cdot\boldsymbol{r}\right)g_1(\boldsymbol{r})\exp\left(-\mathrm{i}\frac{2\pi}{\lambda f_a}\rho\cdot\boldsymbol{r}\right)\right.$$
$$\left.+\int_{R}\mathrm{d}^2\boldsymbol{r}\sqrt{G_3(\xi)}\exp\left(\mathrm{i}\frac{2\pi}{\lambda f_1}\xi\cdot\boldsymbol{r}\right)g_2(\boldsymbol{r})\exp\left(-\mathrm{i}\frac{2\pi}{\lambda f_b}\rho\cdot\boldsymbol{r}\right)\right|^2, \tag{1}$$

where Ξ and R are the aperture areas at planes P_1 and P_2, respectively; ξ, $\boldsymbol{r}$ and ρ are the position vectors at planes P_1, P_2 and P_3, respectively; f_1, f_a and f_b are the focal lengths of lenses L_1, L_a and L_b, respectively. After some algebraic procedures we obtain,

$$I(\rho)=\int_R\int_R g_1(\boldsymbol{r})g_1^*(\boldsymbol{r}')g_3(\boldsymbol{r}-\boldsymbol{r}')\exp\left[-\mathrm{i}\frac{2\pi}{\lambda f_a}\rho\cdot(\boldsymbol{r}-\boldsymbol{r}')\right]\mathrm{d}^2\boldsymbol{r}\,\mathrm{d}^2\boldsymbol{r}'$$
$$+\int_R\int_R g_2(\boldsymbol{r})g_2^*(\boldsymbol{r}')g_3(-\boldsymbol{r}+\boldsymbol{r}')\exp\left[-\mathrm{i}\frac{2\pi}{\lambda f_b}\rho\cdot(\boldsymbol{r}-\boldsymbol{r}')\right]\mathrm{d}^2\boldsymbol{r}\,\mathrm{d}^2\boldsymbol{r}'$$
$$+\int_R\int_R g_1(\boldsymbol{r})g_2^*(\boldsymbol{r}')g_3(\boldsymbol{r}+\boldsymbol{r}')\exp\left[-\mathrm{i}\frac{2\pi}{\lambda}\rho\cdot\left(\frac{\boldsymbol{r}}{f_a}-\frac{\boldsymbol{r}'}{f_b}\right)\right]\mathrm{d}^2\boldsymbol{r}\,\mathrm{d}^2\boldsymbol{r}'$$
$$+\int_R\int_R g_1^*(\boldsymbol{r}')g_2(\boldsymbol{r})g_3(-\boldsymbol{r}-\boldsymbol{r}')\exp\left[-\mathrm{i}\frac{2\pi}{\lambda}\rho\cdot\left(\frac{\boldsymbol{r}}{f_b}-\frac{\boldsymbol{r}'}{f_a}\right)\right]\mathrm{d}^2\boldsymbol{r}\,\mathrm{d}^2\boldsymbol{r}', \tag{2}$$

where, in general, g_3 is a complex function equal to a scaled inverse FT of G_3:

$$g_3(x)=\int_{\Xi}G_3(\xi)\exp\left(\mathrm{i}\frac{2\pi}{\lambda f_1}\xi\cdot x\right)\mathrm{d}\xi. \tag{3}$$

This relation is the well known Van Cittert–Zernike theorem [5] with g_3 considered as the mutual coherence function between two points separated by a distance x in plane P_2.

The intensity distribution given by eq. (1) is recorded as a transparency, and then displayed in the input plane of a conventional coherent 2-f system, equipped by a lens L_3 with focal length f_3. The output distribution, $c(\tilde{\boldsymbol{r}})$, at plane P_4 ($\tilde{\boldsymbol{r}}$ denotes the coordinate of plane P_4) is obtained by performing a FT (with the scale factor $(\lambda f_3)^{-1}$) on $I(\rho)$ given by eq. (2):

$$c(\tilde{\boldsymbol{r}})=g_3\left(\frac{f_a}{f_3}\tilde{\boldsymbol{r}}\right)\int_R g_1(\boldsymbol{r})g_1^*\left(\boldsymbol{r}-\frac{f_a}{f_3}\tilde{\boldsymbol{r}}\right)\mathrm{d}^2\boldsymbol{r}+g_3\left(-\frac{f_b}{f_3}\tilde{\boldsymbol{r}}\right)\int_R g_2(\boldsymbol{r})g_2^*\left(\boldsymbol{r}-\frac{f_b}{f_3}\tilde{\boldsymbol{r}}\right)\mathrm{d}^2\boldsymbol{r}$$
$$+\int_R g_1(\boldsymbol{r})g_2^*\left(\frac{f_b}{f_a}\boldsymbol{r}-\frac{f_b}{f_3}\tilde{\boldsymbol{r}}\right)g_3\left[\left(1+\frac{f_b}{f_a}\right)\boldsymbol{r}-\frac{f_b}{f_3}\tilde{\boldsymbol{r}}\right]\mathrm{d}^2\boldsymbol{r}+\int_R g_2(\boldsymbol{r})g_1^*\left(\frac{f_a}{f_b}\boldsymbol{r}-\frac{f_a}{f_3}\tilde{\boldsymbol{r}}\right)g_3\left[-\left(1+\frac{f_a}{f_b}\right)\boldsymbol{r}+\frac{f_a}{f_3}\tilde{\boldsymbol{r}}\right]\mathrm{d}^2\boldsymbol{r}, \tag{4}$$

The first two terms, located around the origin, can not be separated from each other and thus are of no interest here. We shall mainly be concerned with the other two terms which can be spatially isolated transversally, by introducing a linear phase function, or longitudinally, by using quadratic phase functions [1].

The third and the fourth terms represent a new kind of integral transform which we shall call triplation since it involves three functions. All three functions contained in the third term of eq. (4) may be complex functions, with the restriction that the FT of $g_3(\boldsymbol{r})$, $G_3(\xi)$ should be a positive valued function.

3. The triplation operation

We define the triplation operation by the relation,

$$c(s)\equiv\langle\!\langle g_1, g_2, g_3\rangle\!\rangle_a^b\equiv\int g_1(x)g_2(x-s)g_3(x-as-b)\,\mathrm{d}x. \tag{5}$$

It is easy to show that the triplation is the distribution along the line $t=as+b$ in the triple correlation domain, where the triple correlation is defined by [6]

$$c(s,t) \equiv \int g_1(x) g_2(x-s) g_3(x-t)\, \mathrm{d}x' \,. \tag{6}$$

To see the connection between these definitions and the optical result, we rewrite the third and the fourth terms of eq. (4), with scaled versions of the various functions

$$c_3(\boldsymbol{s}) = \int_{\mathrm{R}} g_1(\boldsymbol{r}) \dot{g}_2^*(\boldsymbol{r}-\boldsymbol{s}) \dot{g}_3\left(\boldsymbol{r} - \frac{f_\mathrm{b}}{f_\mathrm{b}+f_\mathrm{a}}\boldsymbol{s}\right) \mathrm{d}^2\boldsymbol{r}\,, \quad c_4(\tilde{\boldsymbol{s}}) = \int_{\mathrm{R}} g_2(\boldsymbol{r}) \dot{g}_1^*(\boldsymbol{r}-\tilde{\boldsymbol{s}}) \acute{g}_3\left(\boldsymbol{r} - \frac{f_\mathrm{a}}{f_\mathrm{a}+f_\mathrm{b}}\tilde{\boldsymbol{s}}\right) \mathrm{d}^2\boldsymbol{r}\,, \tag{7}$$

where

$$\dot{g}_1(\boldsymbol{r}) = g_1\left(\frac{f_\mathrm{a}}{f_\mathrm{b}}\boldsymbol{r}\right), \quad \dot{g}_2(\boldsymbol{r}) = g_2\left(\frac{f_\mathrm{b}}{f_\mathrm{a}}\boldsymbol{r}\right), \quad \dot{g}_3(\boldsymbol{r}) = g_3\left(\frac{f_\mathrm{a}+f_\mathrm{b}}{f_\mathrm{a}}\boldsymbol{r}\right), \quad \acute{g}_3(\boldsymbol{r}) = g_3\left(\frac{f_\mathrm{a}+f_\mathrm{b}}{f_\mathrm{b}}\boldsymbol{r}\right), \quad \boldsymbol{s} = \frac{f_\mathrm{a}}{f_3}\tilde{\boldsymbol{r}}, \quad \tilde{\boldsymbol{s}} = \frac{f_\mathrm{b}}{f_3}\tilde{\boldsymbol{r}}\,.$$

Obviously, the two terms of eq. (7) are triplation distributions with parameters: $(a, b) = (f_\mathrm{b}/(f_\mathrm{a}+f_\mathrm{b}), 0)$, and $(a, b) = (f_\mathrm{a}/(f_\mathrm{a}+f_\mathrm{b}), 0)$, respectively. In other words, changing the ratio between the focal distances of the two Fourier lenses produces the distributions over planes, each one represented by the equation $\boldsymbol{t} = a\boldsymbol{I}\boldsymbol{s} + \boldsymbol{b}$, where I is the identity matrix, $\boldsymbol{b} = (0, 0)$ and $a = (f_\mathrm{b}/(f_\mathrm{a}+f_\mathrm{b}))$, in the four dimensional triple correlation distribution between three 2D functions. To cover the whole triple-correlation domain by triplation operations we have to scan all slope values by compensating for the scale changes. One way to do this is by a proper imaging system in each channel, that can be independently varied. Alternatively, one may choose a single slope value (single focal lengths ratio) and change gradually the parameter $\boldsymbol{b}$. Changing $\boldsymbol{b}$ can be easily achieved by shifting one of the three functions within its plane.

The spectral distribution of the triplation is derived in the appendix. It is shown that the Fourier transform of a triplation is a triplation too, which operates on the scaled Fourier transform of the original three functions.

$$\mathcal{F}\{\langle\langle g_1, g_2, g_3 \rangle\rangle_\mathrm{a}^\mathrm{b}\} = \frac{1}{1-a} \langle\langle G_1, \mathscr{V}\left[\frac{1}{a-1}\right] G_3^{(\mathrm{b})}, \mathscr{V}\left[\frac{a}{a-1}\right] G_2 \rangle\rangle_{1/\mathrm{a}}^0\,, \quad a \neq 0, 1\,, \tag{8}$$

where $G_3^{(\mathrm{b})}(u) = \exp(-\mathrm{i}2\pi b u)\, G_3(u)$, G_i's are the Fourier transforms of the g_i's and $\mathscr{V}[d]$ is the scaling operator defined by the relation $\mathscr{V}[d]\, G(u) = G(du)$. For the special cases, $a = 0$, or $a = 1$, the triplation degenerates to the conventional correlation integral. However, while the convolution integral can be easily evaluated using the convolution theorem, eq. (8) indicates that such a fast procedure is not applicable for the complete triplation. Therefore, the optical implementation of the triplation has an additional value.

Using the above definitions for the special case where $f_3 = f_\mathrm{a} = f_\mathrm{b} = f$, the complex amplitude distribution in plane P_4, given in eq. (4), can be rewritten in the form,

$$\begin{aligned} c(\tilde{\boldsymbol{r}}) &= g_3(\tilde{\boldsymbol{r}}) g_1(\tilde{\boldsymbol{r}}) \star g_1(\tilde{\boldsymbol{r}}) + g_3(-\tilde{\boldsymbol{r}}) g_2(\tilde{\boldsymbol{r}}) \star g_2(\tilde{\boldsymbol{r}}) \\ &+ \langle\langle g_1(\boldsymbol{r}), g_2^*(\boldsymbol{r}), \mathscr{V}[2] g_3(\boldsymbol{r}) \rangle\rangle_{1/2}^0 + \langle\langle g_2(\boldsymbol{r}), g_1^*(\boldsymbol{r}), \mathscr{V}[-2] g_3(\boldsymbol{r}) \rangle\rangle_{1/2}^0 \\ &= g_3(\tilde{\boldsymbol{r}}) \int_{\mathrm{R}} g_1(\boldsymbol{r}) g_1^*(\boldsymbol{r}-\tilde{\boldsymbol{r}})\, \mathrm{d}^2\boldsymbol{r} + g_3(-\tilde{\boldsymbol{r}}) \int_{\mathrm{R}} g_2(\boldsymbol{r}) g_2^*(\boldsymbol{r}-\tilde{\boldsymbol{r}})\, \mathrm{d}^2\boldsymbol{r} \\ &+ \int_{\mathrm{R}} g_1(\boldsymbol{r}) g_2^*(\boldsymbol{r}-\tilde{\boldsymbol{r}}) g_3(2\boldsymbol{r}-\tilde{\boldsymbol{r}})\, \mathrm{d}^2\boldsymbol{r} + \int_{\mathrm{R}} g_2(\boldsymbol{r}) g_1^*(\boldsymbol{r}-\tilde{\boldsymbol{r}}) g_3(-2\boldsymbol{r}+\tilde{\boldsymbol{r}})\, \mathrm{d}^2\boldsymbol{r}\,, \end{aligned} \tag{9}$$

where $\star$ denotes correlation. Following eqs. (8) and (9), the intensity distribution in plane P_3, given in eq. (1), can be rewritten in the form

$$\begin{aligned} I(\boldsymbol{u}) &= G_3(\boldsymbol{u}) * |G_1(\boldsymbol{u})|^2 + G_3(-\boldsymbol{u}) * |G_2(\boldsymbol{u})|^2 \\ &+ \langle\langle G_1(\boldsymbol{u}), G_3(-\boldsymbol{u}), G_2^*(-\boldsymbol{u}) \rangle\rangle_2^0 + \langle\langle G_2(\boldsymbol{u}), G_3(\boldsymbol{u}), G_1^*(-\boldsymbol{u}) \rangle\rangle_2^0 \\ &= \int G_3(\boldsymbol{u}') |G_1(\boldsymbol{u}-\boldsymbol{u}')|^2\, \mathrm{d}^2\boldsymbol{u}' + \int G_3(-\boldsymbol{u}') |G_2(\boldsymbol{u}-\boldsymbol{u}')|^2\, \mathrm{d}^2\boldsymbol{u}' \\ &+ \int G_1(\boldsymbol{u}') G_3(\boldsymbol{u}-\boldsymbol{u}') G_2^*(2\boldsymbol{u}-\boldsymbol{u}')\, \mathrm{d}^2\boldsymbol{u}' + \int G_2(\boldsymbol{u}') G_3(\boldsymbol{u}'-\boldsymbol{u}) G_1^*(2\boldsymbol{u}-\boldsymbol{u}')\, \mathrm{d}^2\boldsymbol{u}'\,, \end{aligned} \tag{10}$$

where * is the convolution sign, and $\boldsymbol{u}$ is equal to $\rho/\lambda f$. As we see from eqs. (10) and (9), the optical system generates now the special triplation with $(a, b) = (1/2, 0)$ in the output reconstruction plane and $(a, b) = (2, 0)$ in the Fourier plane.

4. Triplator as a signal processing system

To investigate an interesting possible application of the triplator we define a system by a characteristic function, $h(x)$, which transforms an input signal $g(x)$ to an output $o(x')$ according to the relation,

$$o(x') = \int g\left(\frac{x+x'}{2}\right) g^*\left(\frac{x'-x}{2}\right) h(x)\, \mathrm{d}x\,. \tag{11}$$

This output result is directly obtained for 2D functions from the third term of eq. (9) if we set $g_2(\boldsymbol{r}) = g_1(-\boldsymbol{r}) = g(\boldsymbol{r})$, and the integration variable is changed properly. In other words, the proposed optical system implements the signal processor as defined by eq. (11).

Although the triplation, in the form of eq. (11), is not linear with respect to the input function, g, it maintains some characteristics of linearity, which we shall call weak linearity (WL), which has practical significance for signal processing. The WL operation is defined for a set of functions $g_i(x)$ and an additional function $h(x)$, all having finite extent. If the separation among the functions $g_i(x)$ is large enough so that $h(x)$ can be placed between any two input functions $g_i(x)$'s without overlap, an operation $\mathscr{S}$ is defined as WL operation if the relation,

$$\mathscr{S}\left\{\sum_i A_i g_i(x-d_i)\right\} = \sum_i \mathscr{S}\{A_i g_i(x-d_i)\}\,, \tag{12}$$

is satisfied with d_i being the distance of $g_i(x)$ from the origin (A_i's are constants).

It is easy to show that triplation, as defined in eq. (11), is a WL operation and also shift invariant.

$$\begin{aligned} &\int \left[\sum_i A_i g_i\left(\frac{x+x'}{2} - d_i\right)\right]\left[\sum_j A_j^* g_j^*\left(\frac{x'-x}{2} + d_j\right)\right] h(x)\, \mathrm{d}x \\ &= \sum_i \int A_i g_i\left(\frac{x+x'}{2} - d_i\right) A_i^* g_i^*\left(\frac{x'-x}{2} + d_i\right) h(x)\, \mathrm{d}x = \sum_i |A_i|^2 o_i(x'-2d_i)\,, \end{aligned} \tag{13}$$

where $o_i(x')$ is defined in eq. (11) for the ith input, and crossterms were dropped by the non-overlapping condition. Since in many cases practical signals satisfy the conditions for WL operation, the triplation transform may prove quite useful for signal processing applications. An interesting example is pattern recognition under certain conditions.

A substantial difference exists between correlation and triplation. In the former, the extent of non-zero values in the output is the sum of the extent of the input function plus the extent of the system impulse response, $h(x)$. In the latter, the extent is twice that of the input function and does not depend on $h(x)$. This property

may be useful for cases when the impulse response function is wider than the input signal.

In many cases of pattern recognition algorithms [7] the impulse response function is wider than some of the objects in the training set. However, in these algorithms the meaningful part of the output result is the value of the correlation peak. The usual design goal of these pattern recognition systems is to obtain high and sharp correlation peaks, indicating recognition, and object location. The following simple example demonstrates the

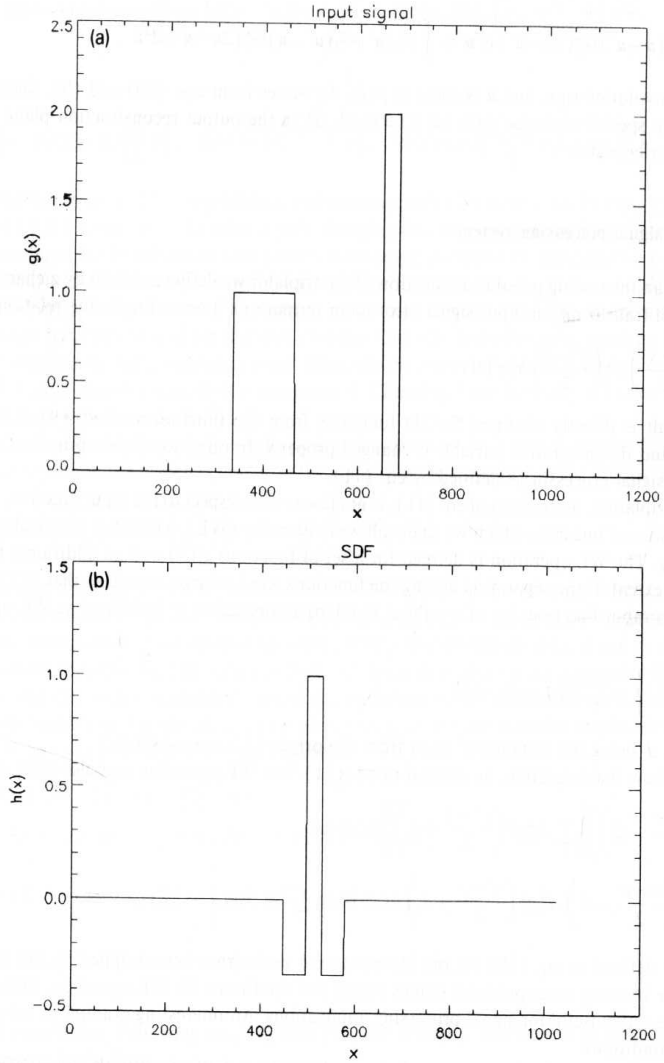

Fig. 2. Comparison of signal matching operation between a conventional correlator and the triplator. (a) The input signals to both system. (b) The SDF, calculated to identify the tall rectangle. (c) The correlation result between the input signals and the SDF. (d) The triplation result obtained with the same input signals and SDF.

superior performance of the triplator over the conventional correlator with respect to correlation peak sharpness.

Let the two rectangles, shown in fig. 2a, be two 1D signals in a given training set. Assume that the aim is to identify the higher rectangle using a synthetic discriminant function (SDF) [8] as shown in fig. 2b. The conventional correlation result between the SDF and the input signal is given in fig. 2c. Taking the same SDF for $h(x)$ and performing a triplation on the same input function generated the output distribution shown in fig. 2d. Although both processes detected the higher rectangle, the triplation peak is much narrower. Note that

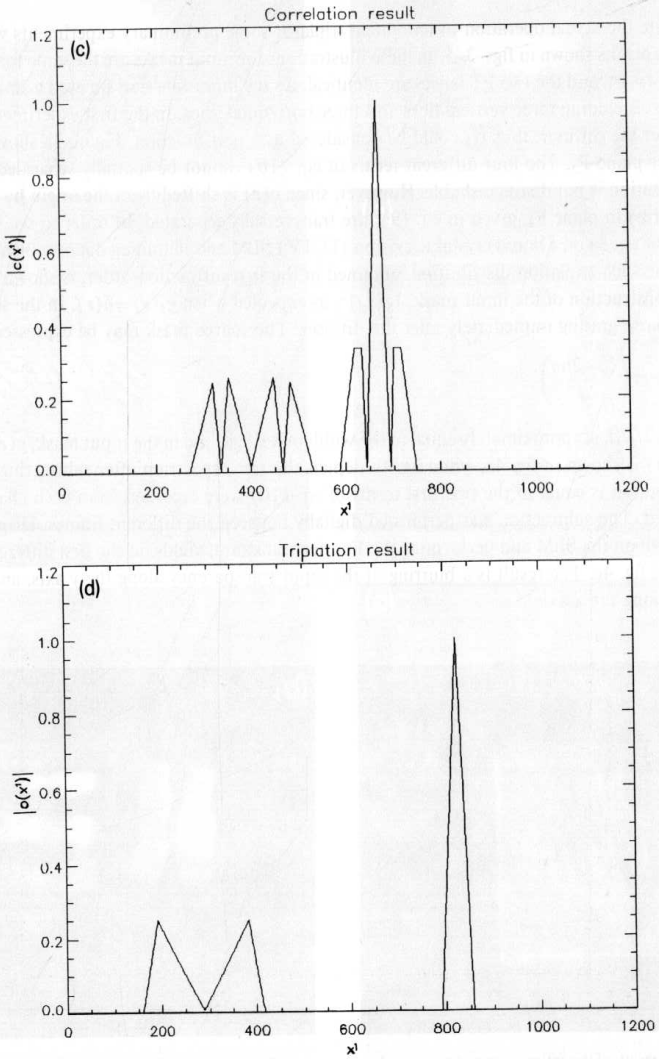

Fig. 2. (Continued.)

the triplation operation produced an output distribution with a separation between the two cross-triplations, twice as large as that between the two crosscorrelation peaks. This makes the effective width of the triplation peak narrower by an additional factor of two. It is expected that filters prepared for triplation will perform even better, but this subject is already outside the scope of this paper.

5. Experimental results

To demonstrate the actual operation of an optical triplator some preliminary experiments were performed with some of the results shown in figs. 3–5. In these illustrations the input masks are the same for both channels, $g(\boldsymbol{r})=g_1(\boldsymbol{r})=g_2(-\boldsymbol{r})$, and the two FT lenses are identical. As the input function we used a small section from a resolution chart including three vertical lines and three horizontal lines. In the first experiment there was no source mask after the diffuser, thus G_3 could be considered as a unit function. Figure 3a shows the intensity distribution over plane P_3. The four different terms of eq. (10) cannot be spatially separated, therefore the triplation distribution is not distinguishable. However, since $g(\boldsymbol{r})$ is shifted from the origin by some distance, the triplation terms in plane P_4, given in eq. (9), are transversally separated. In order to see it we displayed the distribution of fig. 3a on a liquid crystal television (LCTV) SLM and illuminated it by a plane wave through a 2-f system. One such triplation distribution, obtained in the first diffraction order, is shown in fig. 3b. The result is the reconstruction of the input mask, $|g(\boldsymbol{r})|^2$, as expected when $g_3(\boldsymbol{r})=\delta(\boldsymbol{r})$. In the second example we inserted a coarse grating immediately after the diffuser. The source mask may be expressed, this time, as

$$G_3(\xi_x, \xi_y)=\sum_n \operatorname{rect}\left(\frac{\xi_y-2nd}{d}\right), \tag{14}$$

where the width, $\lambda f_1/d$, is approximately equal to the width of a single line in the input mask, $g(\boldsymbol{r})$. The spectral distribution, $I(\boldsymbol{u})$ is shown in fig. 4a, while fig. 4b depicts the same spectrum after subtracting the bias term. This bias distribution is equal to the two first terms of eq. (10) were recorded from each channel while the other was blocked. The subtraction was performed digitally between the different frames. Displaying the distribution of fig. 4b on the SLM and performing the Fourier transform, yields, in the first diffraction order, the pattern shown in fig. 4c. The result is a blurring of the input transparency along the y axis, and a reasonable reconstruction along the x axis.

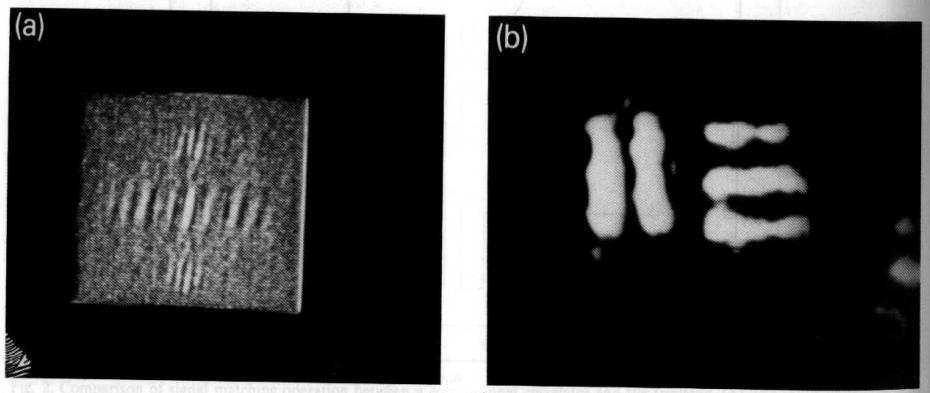

Fig. 3. Experimental results of the optical system obtained without source mask and with a small section of a bar chart as the input masks. (a) The intensity distribution over plane P_3. (b) The triplation distribution measured in a part of plane P_4.

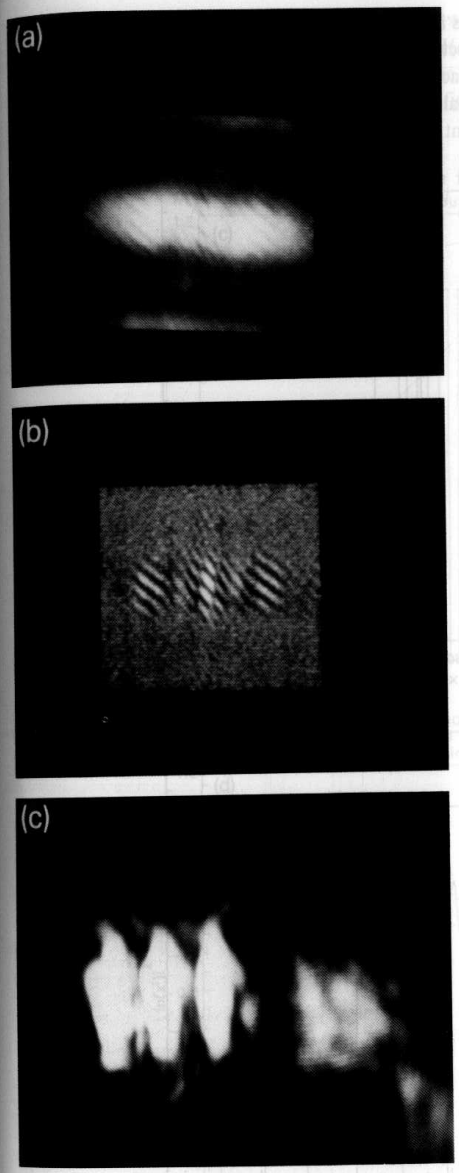

Fig. 4. Experimental results of the optical system obtained with a centered grating as a source mask and with the same input masks as in fig. 3. (a) The intensity distribution over plane P_3. (b) The intensity distribution displayed on the SLM, after subtracting the bias terms. (c) The triplation distribution measured in a part of the plane P_4.

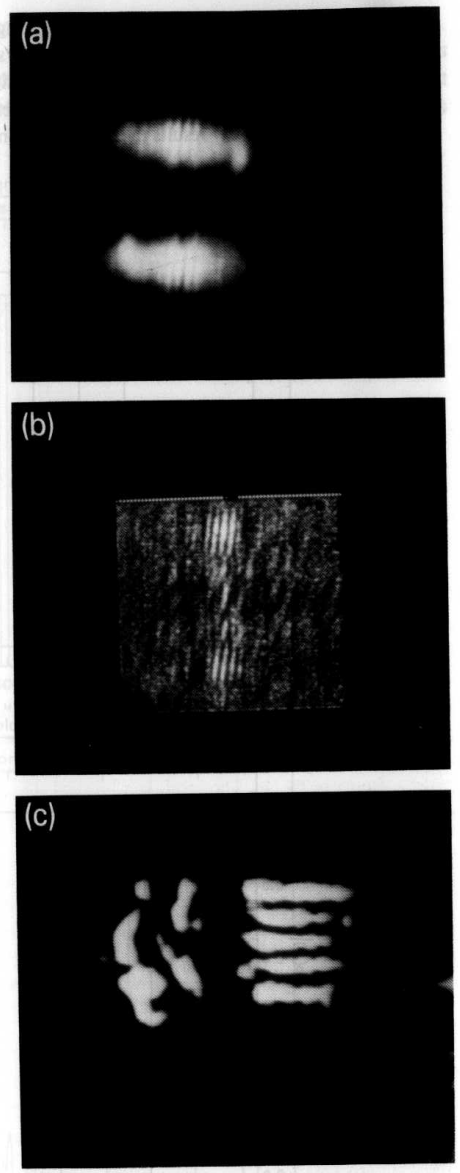

Fig. 5. Experimental results of the optical system obtained with a shifted grating as a source mask and with the same input masks as in fig. 3. (a) The intensity distribution over the plane P_3. (b) The intensity distribution displayed on the SLM, after subtracting the bias terms. (c) The triplation distribution measured in a part of the plane P_4.

In the last demonstration we used the same grating as for the source mask but shifted it by a distance d in the ξ_y direction. As before, figs. 5a, b and c show the spectral distribution, the spectrum without the bias functions and the final output distribution in the first diffraction order of plane P_4, respectively. The triplation, results, shown in figs. 5c, illustrates edge enhancement along the y direction.

To support the laboratory results the above experiment was repeated by computer simulation using 1D signals. The input signal $g(x)$, and the triplation result, when $H(u) = \mathcal{F}\{h(x)\} = G_3(u) = \text{const.}$ are shown in figs. 6a and b, respectively. The second tested function $H(u)$, and the output result, with the same input (fig. 6a), are depicted in figs. 6c and d, respectively. Finally, the same grating of fig. 6c is shifted by a half cycle, as shown in fig. 6e. The consequential output result appears in fig. 6f. All these triplation results indicate similar behavior to the optical experimental results.

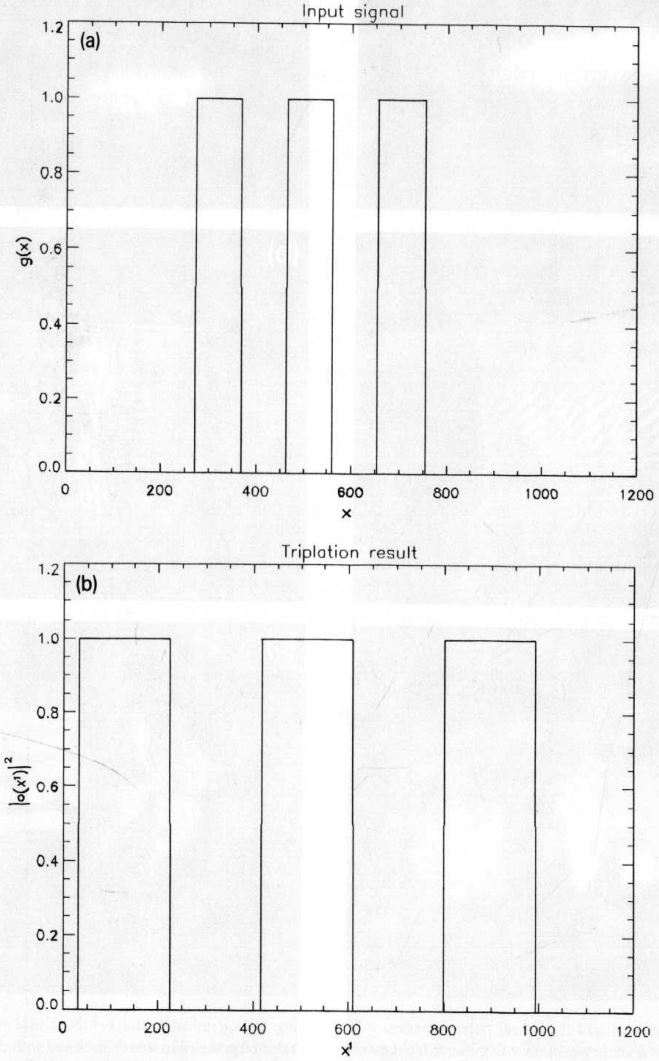

Fig. 6. Simulation results of the 1D triplator. (a) The input signal. (b) The output distribution when the source mask is equal to constant. (c) Another example of a source mask. (d) The triplation result with the function shown in (c). (d) The same source mask as in (c) but shifted a half cycle. (e) The triplation result with the function shown in (d).

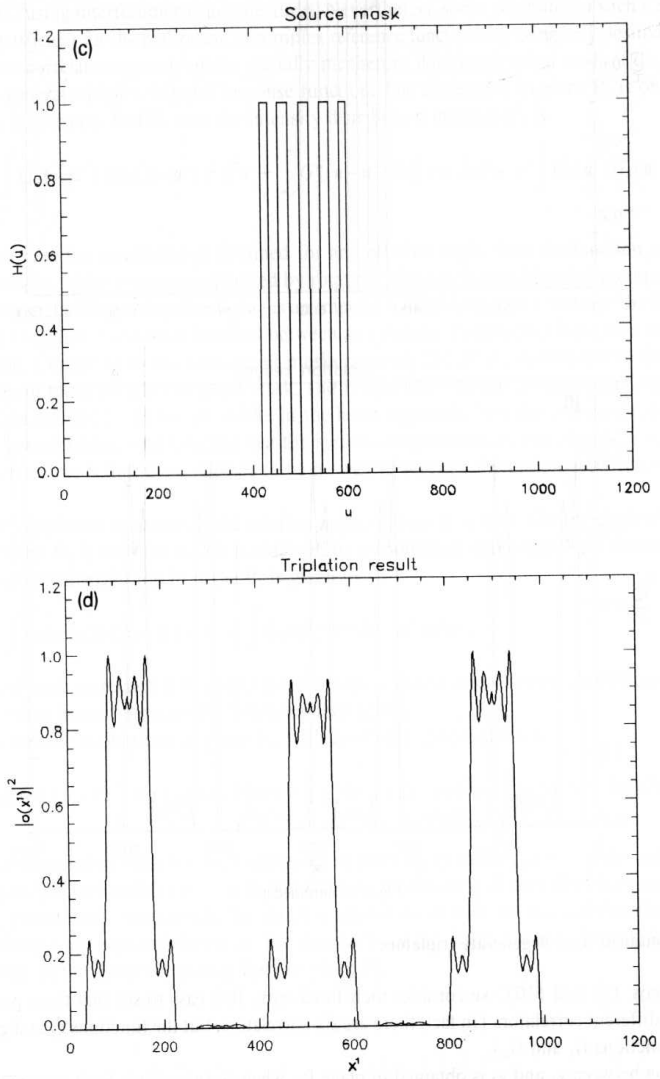

Fig. 6. (Continued.)

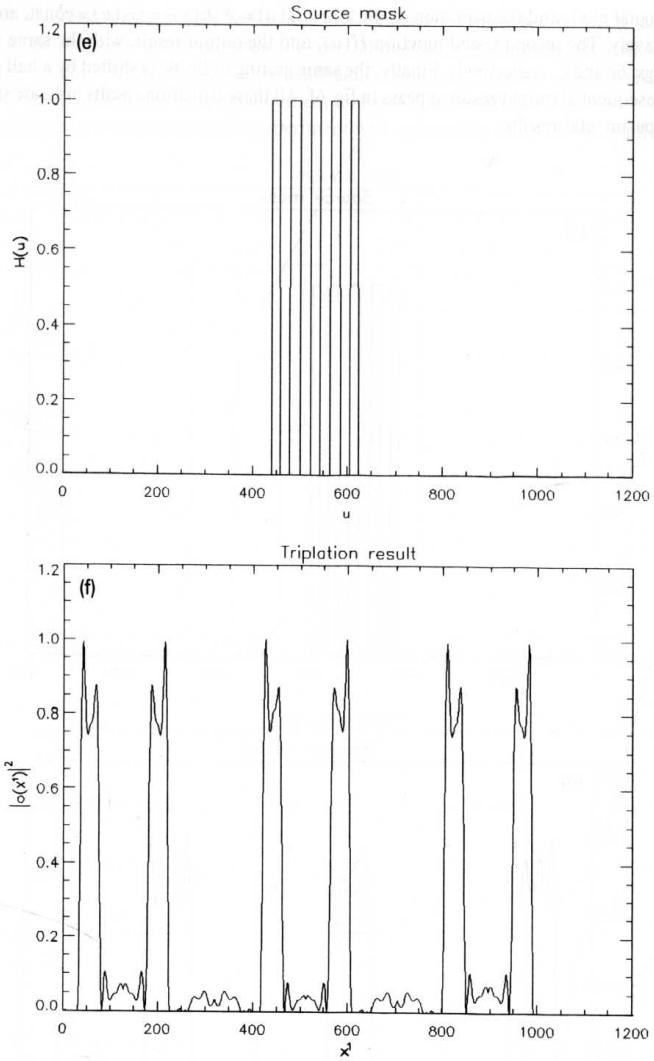

Fig. 6. (Continued.)

6. Correlators obtained from degenerate triplators

Returning to eqs. (9) and (10), we consider their third term. It is easy to see that these processors can be reduced to four different correlators (in fact, there are six correlators, but the functions g_1 and g_2 are analogues as well as the functions G_1 and G_2).

The correlation between g_1 and g_2 is obtained in plane P_4, when $G_3(\boldsymbol{u})=\delta(\boldsymbol{u})$. Such a source mask converts the system into a coherent one, and therefore this correlator is the classical coherent JTC [2]. Since it is a

coherently illuminated system the rotation angle between the interferometer channels has no longer a physical meaning. The output distribution over plane P_4 becomes

$$c(\tilde{\boldsymbol{r}})=\int_R g_1(\boldsymbol{r})g_1^*(\boldsymbol{r}-\tilde{\boldsymbol{r}})\,\mathrm{d}^2\boldsymbol{r}+\int_R g_2(\boldsymbol{r})g_2^*(\boldsymbol{r}-\tilde{\boldsymbol{r}})\,\mathrm{d}^2\boldsymbol{r}+\int_R g_1(\boldsymbol{r})g_2(\boldsymbol{r}-\tilde{\boldsymbol{r}})\,\mathrm{d}^2\boldsymbol{r}+\int_R g_2(\boldsymbol{r})g_1^*(\boldsymbol{r}-\tilde{\boldsymbol{r}})\,\mathrm{d}^2\boldsymbol{r}\,, \tag{15}$$

with the last two terms representing the proper correlation distribution. There is no obvious advantage in implementing a JTC using interferometric architectures. Nevertheless, some attributes of such a system are now under study, in particular for the realization of complex reference functions by using only positive valued masks.

The other three correlators operate under spatially incoherent illumination and in all of them it is possible to implement a general complex impulse response function. The correlation in plane P_3 is obtained between G_2 and G_3 if G_1 is constant. In this case the intensity distribution in plane P_3 is

$$I(\boldsymbol{u})=\text{const.}+\int \mathrm{G}_3(-\boldsymbol{u}')\,|G_2(\boldsymbol{u}-\boldsymbol{u}')|^2\,\mathrm{d}^2\boldsymbol{u}'+\int G_2^*(\boldsymbol{u}-\boldsymbol{u}')G_3(-\boldsymbol{u}')\,\mathrm{d}^2\boldsymbol{u}'+\int G_2(\boldsymbol{u}')G_3(\boldsymbol{u}'-\boldsymbol{u})\,\mathrm{d}^2\boldsymbol{u}'\,. \tag{16}$$

In this particular case the correlation is obtained for any rotation angle since the function g_1 is just a delta function at the origin, which remains unchanged by rotation. If $G_3(\boldsymbol{u})$ is considered as an input function, and $g_2(\boldsymbol{r})$ is taken as a spatial filter (therefore $G_2(\boldsymbol{u})$ is an impulse response function), then the third (or the fourth) term of eq. (16) yields a correlation function between an intensity distribution input to a complex impulse response function. Compared to the multi pupil masks methods [9] of incoherent spatial filtering, this proposed configuration requires only one pupil mask, and is equivalent in the complexity to one of Leith's correlators (case 2 in ref. [10]). However, unlike in the latter approach, here the correlation is done on an irradiance input transmittance, which means that the system can processes diffuse objects as well. A drawback of both these correlators is that there appears to be no way to separate the undesired terms of eq. (16) from the third term.

The two other correlators exist only if the rotation angle is larger then zero. The correlation between G_1 and G_2 is obtained when G_3 is constant which is obtained by a completely incoherent light source in plane P_1. In this case the intensity distribution in plane P_3 is given by

$$I(\boldsymbol{u})=\text{const.}+\int G_1(\boldsymbol{u}')G_2^*(2\boldsymbol{u}-\boldsymbol{u}')\,\mathrm{d}^2\boldsymbol{u}'+\int G_2(\boldsymbol{u}')G_1^*(2\boldsymbol{u}-\boldsymbol{u}')\,\mathrm{d}^2\boldsymbol{u}'\,. \tag{17}$$

The usefulness of such correlator is not clear since it makes a correlation between the Fourier transforms of both input functions instead between the functions themselves.

The fourth correlator is obtained in plane P_4, with $g_1=\text{const.}$, and is given by

$$c(\tilde{\boldsymbol{r}})=g_3(\tilde{\boldsymbol{r}})\,\text{const.}+g_3(-\tilde{\boldsymbol{r}})\int_R g_2(\boldsymbol{r})g_2^*(\boldsymbol{r}-\tilde{\boldsymbol{r}})\,\mathrm{d}^2\boldsymbol{r}+\int_R g_2^*(\boldsymbol{r})g_3(2\boldsymbol{r}+\tilde{\boldsymbol{r}})\,\mathrm{d}^2\boldsymbol{r}+\int_R g_2(\boldsymbol{r})g_3(-2\boldsymbol{r}+\tilde{\boldsymbol{r}})\,\mathrm{d}^2\boldsymbol{r}\,. \tag{18}$$

The two last correlation terms can be easily separated in plane P_4 by shifting g_2 out of the origin. Considering $g_2(\boldsymbol{r})$ as the input function and $G_3(\boldsymbol{u})$ as a spatial filter, a correlation is obtained between two complex functions, although illuminated incoherently. To obtain a similar result with the method described in ref. [9], 6 different pupil masks are required. However, the drawbacks of this correlator mainly come from the low diffraction efficiency of the spectrum grating $I(\boldsymbol{u})$ in plane P_3.

7. Conclusion

A new integral transform, the triplator, was introduced and implemented optically. Mathematically, distin-

guishable feature of the triplation is that the transform to the Fourier domain yields a triplation too (eq. (8)). Implementations of this operation in the field of image processing are currently under intensive investigation.

In principle, a sequence of such transforms can be used to generate the whole domain of a triple correlation. As far as we know, optical implementation of the triple correlation between 2D functions has never been done yet. The applications of the triple correlation in the signal processing field are well summarized in ref. [6], and we would only like to mention that the triple correlation is a generalization of an extended family of transforms and representations, like ambiguity function, Wigner distribution, etc. That means that the proposed system may be used as an analog computer for many mathematical operations.

The triplator itself can be used for signal processing, similar to the conventional correlator, but with unique properties, such as sharp identification peaks in pattern recognition schemes. Degeneration of the triplation yields a collection of correlators, out of which three may be useful for incoherently illuminated correlation between complex functions.

In the experimental work we demonstrated the feasibility of implementation using some simple examples. Of course, the results for these simple cases could be also derived by conventional spatial filtering. However, the two procedures are substantially different and the triplation operation has additional possibilities. Some of these were indicated here while others are still under investigation.

Acknowledgements

This work was done while J. Rosen held a National Research Council–Rome Laboratory Research Associateship.

Appendix

In this appendix we derive the relation between the triplation in the image domain to its distribution in the spectral domain. To simplify the notation we use 1D functions. The Fourier transform of the triplation function, given in eq. 5, is

$$C(\tilde{u}) = \mathcal{F}\{c(\tilde{r})\} = \iint g_1(r) g_2(r-\tilde{r}) g_3(r-a\tilde{r}-b) \exp(-i2\pi\tilde{u}\tilde{r})\, dr\, d\tilde{r}$$

$$= -\int dr\, g_1(r) \exp(-i2\pi\tilde{u}r) \int dy\, g_2(y) g_3[r(1-a)+ay-b] \exp(i2\pi\tilde{u}y)$$

$$= -\int dr\, g_1(r) \exp(-i2\pi\tilde{u}r) \int du \exp(i2\pi ur) \int dr \exp(-i2\pi ur)$$

$$\times \int dy\, g_2(y) g_3[r(1-a)+ay-b] \exp(i2\pi\tilde{u}y)$$

$$= -\int dr\, g_1(r) \exp(-i2\pi\tilde{u}r) \int du \exp(i2\pi ur) \int dy\, g_2(y) \exp(i2\pi\tilde{u}y)$$

$$\times \int dr\, g_3[r(1-a)+ay-b] \exp(-i2\pi ur)$$

$$= \frac{1}{a-1} \int dr\, g_1(r) \exp(-i2\pi\tilde{u}r) \int du \exp\left[i2\pi\left(r - \frac{b}{1-a}\right)u\right] G_3\left(\frac{u}{1-a}\right) \int dy\, g_2(y) \exp\left[i2\pi\left(\tilde{u} + \frac{au}{1-a}\right)y\right]$$

$$= \frac{1}{a-1} \int dr\, g_1(r) \exp(-i2\pi\tilde{u}r) \int du \exp\left[i2\pi\left(r - \frac{b}{1-a}\right)u\right] G_3\left(\frac{u}{1-a}\right) G_2\left(\frac{au}{1-a} + \tilde{u}\right)$$

$$= \frac{1}{a-1} \int du \exp\left(-i2\pi \frac{b}{1-a} u\right) G_3\left(\frac{u}{1-a}\right) G_2\left(\frac{au}{1-a} + \tilde{u}\right) \int dr\, g_1(r) \exp[-i2\pi(\tilde{u}-u)r]$$

$$= \frac{1}{a-1} \int du \exp\left(-i2\pi \frac{b}{1-a} u\right) G_3\left(\frac{u}{1-a}\right) G_2\left(\frac{au}{1-a} + \tilde{u}\right) G_1(\tilde{u}-u)$$

$$= \frac{1}{1-a} \int du \exp\left(-i2\pi \frac{b}{a-1} (u-\tilde{u})\right) G_1(u) G_2\left(\frac{ua}{a-1} - \frac{\tilde{u}}{a-1}\right) G_3\left(\frac{u}{a-1} - \frac{\tilde{u}}{a-1}\right)$$

$$= \frac{1}{1-a} \int du \exp\left(-i2\pi \frac{b}{a-1} (u-\tilde{u})\right) G_1(u) \tilde{G}_3(u-\tilde{u}) \tilde{G}_2(u-\tilde{u}/a)\,, \tag{19}$$

where

$$\tilde{G}_2 = \mathcal{F}\left[\frac{a}{a-1}\right] G_2\,, \quad \tilde{G}_3 = \mathcal{F}\left[\frac{1}{a-1}\right] G_3\,.$$

References

[1] J. Rosen, M. Segev, J. Shamir and A. Yariv, J. Opt. Soc. Am. A 9 (1992) 1498.
[2] C.S. Weaver and J.W. Goodman, Appl. Optics 5 (1966) 1248.
[3] S. Wang and N. George, Appl. Optics 24 (1985) 842.
[4] M. Segev and A. Yariv, Optics Lett. 17 (1992) 145.
[5] M. Born and E. Wolf, Principles of optics (Pergamon, New York, 1980).
[6] A.W. Lohmann and B. Wirnitzer, Proc. IEEE 72 (1984) 889.
[7] B.V.K. Vijaya Kumar, Appl. Optics 31 (1992) 4773; and many references therein.
[8] C.F. Hester and D. Casasent, Appl. Optics 19 (1980) 1758.
[9] I. Glaser, Prog. in Optics, ed. E. Wolf, 24 (1987) 389.
[10] E.N. Leith and D.K. Angell, Appl. Optics 25 (1986) 499.